Hydroecology and Engineering

SCIEPublish

Article

Effects of a Mismatch Between the Water Temperature of Yangtze River and the Specific Requirements of Chinese Sturgeon, *Acipenser sinensis*

Xin'er Ning, Dongshuo Lu and Jianbo Chang *

State Key Laboratory of Water Resources Engineering and Management, Wuhan University, Wuhan 430072, China; xening@whu.edu.cn (X.N.); ludongshuo@whu.edu.cn (D.L.)

* Corresponding author. E-mail: changjb@whu.edu.cn (J.C.)

Received: 29 July 2026; Revised: 11 August 2026; Accepted: 18 September 2026; Available online: 15 October 2026

ABSTRACT: The interruption of natural reproduction in the Chinese sturgeon, *Acipenser sinensis*, is an urgent ecological concern, and the thermal mechanisms underlying its stepped deterioration warrant attention. To systematically elucidate these mechanisms, this study quantified thermal dynamics throughout the reproductive cycle using a multi-scale retrospective analysis of water temperature and historical spawning records. A pronounced, stepwise mismatch between Yangtze River water temperatures and the reproductive requirements of the Chinese sturgeon was identified, manifested as significantly intensified thermal stress and temporal delay. Kernel density estimation (KDE) was used to quantify the thermal requirements for overwintering gonadal development and spawning. Period-stratified statistical tests were then applied to evaluate the alignment between ambient thermal regimes and species-specific requirements. Based on the interdecadal evolution of this mismatch, an intersection analysis between seasonal cooling curves and median spawning temperature was introduced to evaluate synchrony between spawning dates and thermal cues. These analyses revealed that spawning dates passively followed the postponement of the thermal cue, whereas the preferred temperature remained fixed. Collectively, this study demonstrates that thermal mismatches have intensified stepwise through both absolute exceedance of overwintering thresholds and mistimed arrival of suitable spawning temperatures, leading to the sequential degradation of reproduction.

Keywords: Yangtze River; Water temperature; Thermal mismatch; Ecological implication; Chinese sturgeon (*Acipenser sinensis*)

1. Introduction

The Chinese sturgeon is a large river-dwelling anadromous fish whose life cycle encompasses freshwater growth, marine fattening, and upstream spawning. Historically, the species was widely distributed in the mainstream of the Yangtze River and adjacent marine waters, serving as a flagship species of the Yangtze ecosystem [1]. However, since the second half of the 20th century, multiple pressures, including overfishing, shipping disturbance, water pollution, and dam construction, have driven a sharp

© 2026 The authors. This is an open access article under the Creative Commons Attribution 4.0 International License (https://creativecommons.org/licenses/by/4.0/).

population decline [2,3]. In the 1970s, the spawning stock in the Yangtze River was estimated at approximately 10,000 individuals [4], while hydroacoustic surveys conducted during 2014–2017 recorded only 22 to 106 spawning individuals [5]. The construction of the Gezhouba Dam in 1981 blocked its migratory pathway, truncating the original spawning grounds in the lower Jinsha River to an area immediately downstream of the dam in the middle Yangtze River (As shown in Figure S1) [1]. Subsequently, the successive operation of the Three Gorges Project and upstream cascade reservoirs further altered the hydrological regime of the middle and lower Yangtze, causing flow and temperature rhythm to increasingly deviate from the natural conditions to which the species is evolutionarily adapted. Since 2017, no natural spawning has been recorded, and the wild population is now critically endangered [6].

Historical records show that spawning anomalies in the Chinese sturgeon are not monotonically gradual but exhibit a stepped deterioration, from 1–3 spawning events per year with relatively stable timing, to only 0–2 events per year with significantly delayed dates, and finally to complete cessation [5,6]. Two main explanations have been proposed for this reproductive crisis: a drastic decline in the number of mature adults and riverine environmental changes, including the loss of spawning habitat and hydrological alterations [1]. A decrease in population size and spawning habitat would undoubtedly reduce reproductive output, but this can only explain a monotonic declining trend. The stepped pattern of changes in spawning frequency and timing is more consistent with the potential impacts of hydrological regime alterations.

The alignment between life history requirements and ambient habitat conditions is the result of natural selection and evolutionary refinement [7,8]. Organisms have a limited adaptive capacity to respond to abrupt environmental changes [9,10]. For poikilothermic aquatic organisms, water temperature serves as a critical environmental cue ensuring the completion of life history processes. Once thermal regimes shift abruptly beyond the spatiotemporal requirements of a species and exceed its adaptive capacity, they pose a severe threat to survival [11–13].

The reproductive cycle of sturgeons comprises two critical stages that are highly sensitive to temperature: a gonadal development phase that requires a period of low-temperature stimulation to initiate vitellogenesis, and a final maturation and spawning season that must occur within a suitable temperature window [14–18]. Most sturgeons require approximately 2–4 months of cold exposure to promote gonadal maturation [19–21]. Abnormal temperatures may lead to failure of primary oocytes to enter the vitellogenin phase, follicular atresia, and gonadal regression [22–24]. In the Yangtze River, Chinese sturgeon arrive near the spawning grounds to overwinter in the year of their spawning migration, but do not spawn. In the following autumn, as environmental conditions such as water temperature and water level gradually fall within the optimal range for reproduction, the recruitment cohort completes its final gonadal development, matures, and may reproduce [4]. Appropriate temperature during gonadal development and spawning is crucial for successful reproduction.

Existing studies have extensively investigated the thermal requirements of the Chinese sturgeon. Yang et al. reported that spawning temperatures at sites downstream of the Gezhouba Dam and in the Jinsha River ranged between 15–21 °C, concluding that this range is a prerequisite for spawning [25]. Using rare-events logistic regression, Gao et al. suggested that an optimal environmental window of 17–20 °C is required for successful reproduction [26]. Chang et al. defined thermal ranges based on physiological considerations, examined longitudinal water temperature variations in the Yangtze River, and assessed the thermal suitability of locations such as Yichang [27]. Tao et al. further proposed appropriate ranges of air temperature and discharge to maintain suitable water temperatures for Chinese sturgeon spawning [28]. In recent years, the delayed reproduction of the Chinese sturgeon has been increasingly attributed to temperature changes. Shen et al. determined that a 25-day delay in the occurrence of approximately 20 °C water temperatures was significantly correlated with a 26-day delay in spawning onset [29]. Gao et al. noted that the thermal lag effect induced by the Three Gorges Reservoir postponed spawning dates to late November [2], with the first spawning date positively correlated with the first occurrence of 20 °C [3].

Zhang et al. constructed thermal response curves and demonstrated that a 0.2 °C increase in water temperature delays Chinese sturgeon spawning by an average of 2.1 days [30]. In addition, studies have examined the effects of overwintering and spring temperatures. Zhang et al. found that gonadal development of Chinese sturgeon breeding populations was correlated with water temperatures from December to March [31]. Xiao and Duan observed a spring cold delay at the Yichang spawning ground, and noted that the available thermal window during the spawning season extended during 2003–2005 but contracted during 2006–2008 [32].

However, existing knowledge of spawning thermal preference largely remains at the level of static thresholds or mean values. The literature often cites 18–20 °C as a general suitable spawning temperature, but such statistical averages mask temporal information. Moreover, despite widespread attention to optimal thermal thresholds for the spawning season, the thermal requirements for overwintering gonadal development have long been overlooked. An integrated perspective on thermal mismatches across the entire reproductive cycle is lacking, and the temporal synchrony between spawning anomalies and thermal mismatches has not been quantitatively characterized. Reproduction of the Chinese sturgeon is a sequential progression of physiological processes, including overwintering gonadal development, maturation, and spawning. If overwintering low temperature conditions are lost, gonadal development may be impaired, and if autumn cooling is delayed, spawning timing may be compressed or misaligned. Thermal mismatches at the two stages do not occur in isolation, rather they may be amplified along the reproductive chain. Therefore, to elucidate the potential thermal mechanisms underlying these reproductive anomalies and to recognize the species' overlooked thermal requirements, it is necessary to extend the analysis to the entire reproductive cycle, covering the multifaceted needs for spawning.

To address these gaps, this study draws on precise records of natural spawning events from 1982 to 2016 [5,33,34]. It aims to answer the following questions: What are the key water temperature thresholds for overwintering gonadal development and autumn spawning? Facing long-term thermal alterations, has the spawning temperature preference of the Chinese sturgeon remained stable under long-term thermal alteration? Is the delay in spawning dates synchronized with changes in thermal conditions? To this end, kernel density estimation (KDE) was applied to quantify key thresholds, period-stratified statistical tests were used to assess the stability of spawning water temperatures, and an intersection analysis method was introduced to quantify the synchrony between spawning dates and the temporal shift of thermal cues. By integrating the thermal requirements of both the overwintering and spawning stages, this study seeks to reveal the mechanism underlying the synchrony between thermal mismatches and spawning anomalies, elucidate how changes in the Yangtze River thermal regime affect reproductive success through both threshold exceedance and mistimed thermal signals, and provide a scientific basis for developing targeted conservation strategies.

2. Materials and Methods

2.1. Study Area and Data Sources

Daily water temperature records for 1982 to 2023 were obtained from the Yichang Hydrological Station, situated approximately 2 km downstream of the current spawning grounds and considered representative of the thermal conditions at the spawning site. This study focused on two critical life-history periods: the overwintering phase, presumed crucial for gonadal development, and the autumn spawning season.

Spawning dates for 52 natural events between 1982 and 2016 were compiled from field surveys of egg-predatory fishes [33,34] and hydroacoustic monitoring [6,25,35,36] conducted below the Gezhou Dam, with most events occurring from October to November [1]. This species spawns 1–3 times annually. For each year, spawning events were ordered chronologically.

Since spawning timing and frequency after 2002 showed significant delays and declines, this study used the period from 1981 to 2001 to estimate the optimal thermal range for gonadal development, during which the temperature patterns were relatively stable and consistent with historical records. Considering that sturgeons require a low-temperature control period of 2–3 months for overwintering at 4 to 5 °C [19] and given the seasonal temperature cycle of the Yangtze River, the period from January to February was the only and most probable overwintering window. Consequently, the reference period for estimating optimal thresholds for overwintering gonadal development and spawning was defined as January to February and October to November, respectively.

All analyses and visualizations were conducted using Python 3.13.5, MATLAB R2024a. The choice of these software packages is not exclusive, and equivalent tools can be used as substitutes.

2.2. Estimation of Optimal Thermal Ranges for Gonadal Development and Spawning

2.2.1. Data Preparation and Annual Statistical Descriptors

To analyze the overwintering thermal regime, daily water temperature observations for January and February from 1981 to 2001 were extracted. For each year i $(i = 1981, 1982, \dots, 2001)$, the daily temperature series was denoted as $T_i = \{t_{i1}, t_{i2}, \dots, t_{in_i}\}$, where n_i is the number of observation days. Three annual statistical descriptors were calculated: the minimum $\left(Min_i = min(T_i)\right)$, maximum $\left(Max_i = max(T_i)\right)$ and mean $\left(Mean_i = \frac{1}{n_i}\sum_{j=1}^{n_i} t_{ij}\right)$ overwintering temperatures. For each descriptor, the overall value range $[min(M), max(M)]$ and mean value $(\mu_{Min}, \mu_{Mean}, \mu_{Max})$ were computed. However, owing to a progressive backward shift of the cool thermal zone in the long-term evolution of overwintering temperatures (Ning, unpublished), the critical window for overwintering development after 2003 may have effectively extended into February–March. Accordingly, for the long term assessment of thermal mismatch, the overwintering observation period was expanded to January–March to capture thermal stress risks more comprehensively.

For the spawning analysis, a separate dataset was constructed. Each documented spawning date (derived from the field records described in Section 2.1) was paired with its corresponding daily water temperature measured at the Yichang hydrological station, forming the spawning temperature dataset $T_s = \{T_1, T_2, \dots, T_{53}\}$.

2.2.2. Estimation of Probability Density

The non-parametric kernel density estimation (KDE) method [37,38] was employed to model the probability density functions (PDFs) of the temperature datasets. For a generic dataset $X = \{x_1, x_2, \dots, x_m\}$ containing m independent samples, the estimated PDF $\hat{f}(x)$ is:

$$\hat{f}(x) = \frac{1}{mh}\sum_{i=1}^{m} K\left(\frac{x - x_i}{h}\right)$$

where $K\left(\frac{x - x_i}{h}\right)$ is the kernel function. This study employed the standard Gaussian kernel function: $K(u) = \frac{1}{\sqrt{2\pi}} e^{-\frac{1}{2}u^2}$. The bandwidth $h > 0$, which controls the smoothness of the PDF curve, was automatically determined using Scott's rule [39].

2.2.3. Key Temperature Thresholds for Gonadal Development

The KDE method was applied to the set of annual mean overwintering temperatures $\{Mean_i\}$ to construct its probability density distribution. The following key boundaries for gonadal development were derived:

(1) Low Boundary (L): $L = min(\{Mean_i\})$
(2) Optimal Boundary (O): $O = \mu_{Mean}$ (the mean of the set $\{Mean_i\}$)
(3) High Boundary (H): $H = max(\{Mean_i\})$

These establish the estimated lower boundary, central tendency, and upper boundary of the optimal thermal range for overwintering gonadal development.

Additionally, the absolute maximum water temperature recorded across all January–February days from 1981 to 2001 was identified as a critical upper threshold beyond which gonadal development may be impaired: $T_{max} = max(T_{Jan.-Feb.})$. $T_{Jan.-Feb.}$ denotes the set of daily January–February observations.

2.2.4. Key Temperature Thresholds for Spawning

The probability density distribution of the spawning temperature was based on dataset Ts. The optimal range for spawning was defined as $T_{Spwan} = [min(T_s), T_{Max}]$ with the central tendency characterized by T_{Med}. Two key metrics were derived:

(1) Median Optimal Temperature (T_{Med}): The temperature at which the KDE-derived PDF of Ts attains its maximum value, representing the central tendency at which spawning events are most likely to occur.
(2) Upper Thermal Limit (T_{Max}): The empirical maximum temperature within Ts, serving as the inferred upper threshold at which spawning activity can occur.

2.3. Statistical Analysis of Thermal and Spawning Regimes Across Periods

2.3.1. Characterization of Daily Thermal Environments

Based on documented shifts in the thermal and spawning regimes, the study period was stratified into three distinct periods: P1 (1982–1997), P2 (1998–2005), and P3 (2006–2016). The analysis focused on the spawning season, defined as October–November (approximately day of year, DOY, 274–334).

For each thermal period $p \in \{\mathrm{P1}, \mathrm{P2}, \mathrm{P3}\}$ and for each day d within the seasonal window, the 25th ($Q_{p,d}(0.25)$), 50th ($Q_{p,d}(0.5)$), and 75th ($Q_{p,d}(0.75)$) quantiles of daily water temperatures were calculated from the historical records. These quantiles defined, for each period, a median daily temperature trajectory ($Q_{p,d}(0.50)$) and an interquartile range (IQR) band ($Q_{p,d}(0.25), Q_{p,d}(0.75)$) representing the central 50% of thermal variability.

To provide a reference of recent thermal conditions after the last natural spawning, an additional period P4 (2017–2023) was included for daily water temperature comparisons. Pairwise Mann-Whitney U tests were performed on daily water temperatures within the October–November window across all four periods to evaluate long-term warming trends [40]. Linear regression (ordinary least squares) was applied to spawning water temperatures against year to quantify the long-term trend.

2.3.2. Statistical Comparison of Period-Specific Spawning Characteristics

For the spawning events within each period p, the following descriptive statistics were calculated separately for the date (in DOY) and the spawning water temperature T_s:

(1) Mean ($\overline{x_p}$) and its 95% confidence interval (estimated using the t-distribution).
(2) Median ($\widetilde{x_p}$) its interquartile range ($IQR_p = Q_p(0.75) - Q_p(0.25)$).

To assess whether spawning timing or temperature differed significantly among the three periods, pairwise non-parametric comparisons were conducted using the two-sided Mann-Whitney U test. The test was applied separately to spawning DOY and spawning temperature datasets for the three comparisons: P1 *vs*. P2, P1 *vs*. P3, and P2 *vs*. P3, with a significance level of α = 0.05.

2.3.3. Intersection Analysis of Thermal Trajectories and Spawning Characteristics

To investigate the synchrony between seasonal cooling and spawning activity, this study identified for each period the date when the period's median daily temperature trajectory ($Q_{p,d}(0.5)$) declined to the median spawning temperature ($\widetilde{T_s^p}$). The intersection date d_p^* was determined by:

(1) Identifying consecutive days d_i and d_{i+1} where the median temperature curve crossed the threshold $\widetilde{T_s^p}$, satisfying: $\left[Q_{p,d_i}(0.50) - \widetilde{T_s^p}\right] \times \left[Q_{p,d_{i+1}}(0.50) - \widetilde{T_s^p}\right] \leq 0$.

(2) Calculating the precise intersection date by linear interpolation:

$$d_p^* = d_i + \frac{\widetilde{T_s^p} - Q_{p,d_i}(0.50)}{Q_{p,d_{i+1}}(0.50) - Q_{p,d_i}(0.50)} \times (d_{i+1} - d_i)$$

This metric d_p^* estimates the calendar date when ambient thermal conditions match the period-specific spawning temperature, providing a standardized measure for quantifying the synchrony from environmental thermal cues and spawning timing.

3. Result

3.1. Overall Characteristics of Spawning Date and Water Temperature

From 1982 to 2016, the natural reproduction in Chinese sturgeon exhibited a stepped deterioration. Historical records show that prior to 2003, spawning occurred 1–3 times annually, with the first spawning event typically occurring from mid- to late October. After 2003, annual spawning frequency dropped to 0–2 times. After 2006, the first spawning date shifted to late November. The first interruption occurred in 2013, again in 2015, and no spawning has been recorded since 2017 (Figure 1).

During 1982–1997, the first spawning date showed considerable interannual variation in the 1980s, but multiple spawning events (second and third) were still observed. In the 1990s, spawning dates became more stable, possibly reflecting the gradual establishment of a regular spawning pattern at the new grounds. The period 1998–2005 served as a transition, with the first spawning date shifting progressively later and the second spawning events becoming infrequent after 2002. From 2006 to 2016, spawning occurred consistently in late November, and except for 2012, only one or no spawning event was recorded per year.

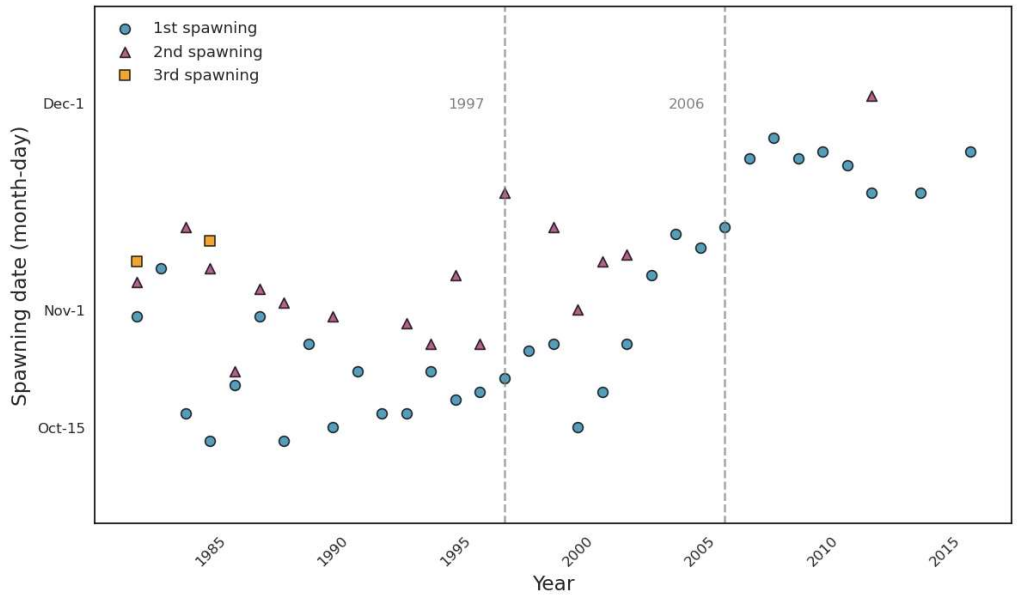


Figure 1. Interannual variation of spawning dates. Different symbols denote the order of spawning events (first, second, third, and fourth or more). Vertical dashed lines indicate the transition years 1997 and 2006.

Over the study period, spawning water temperature exhibited a gradual warming trend (slope ≈ 0.0311 °C·yr^{-1}) over the study period, without marked interannual shifts comparable to those observed for spawning dates or frequency (Figure 2).

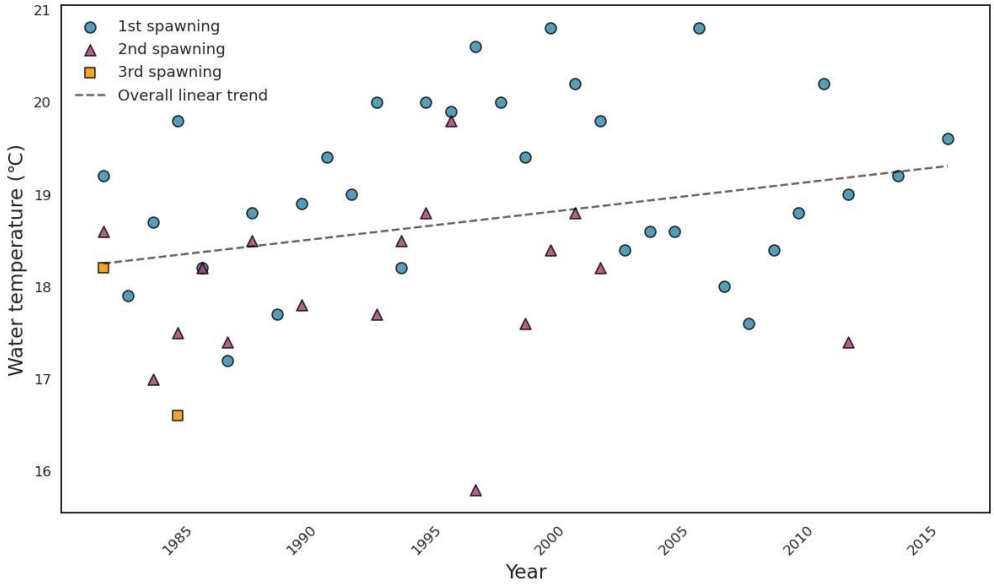
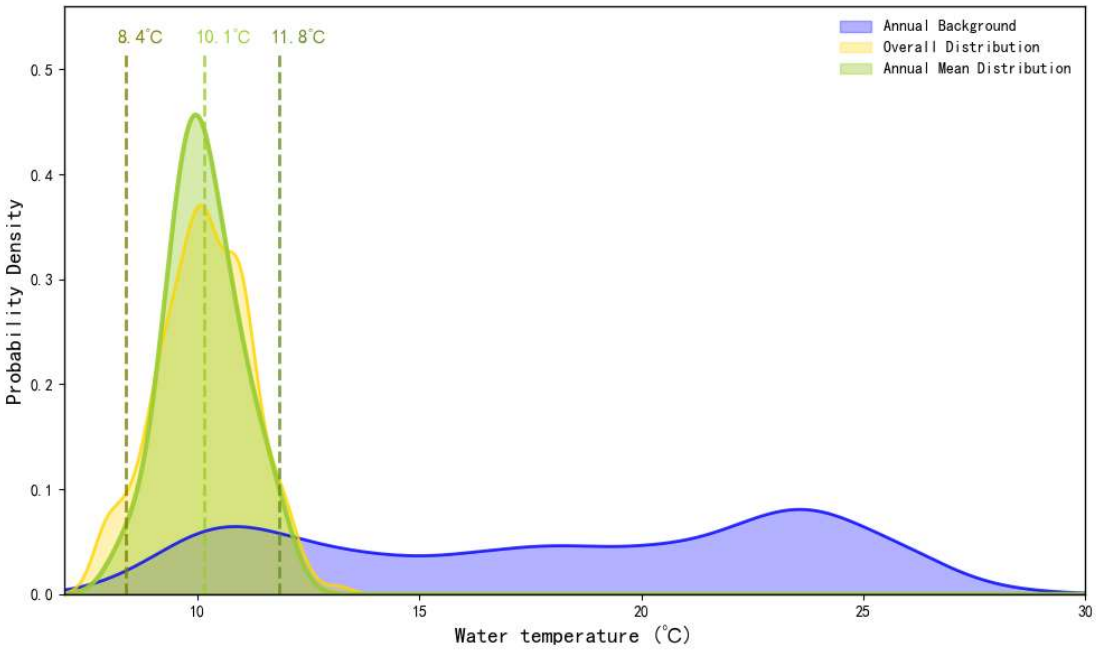


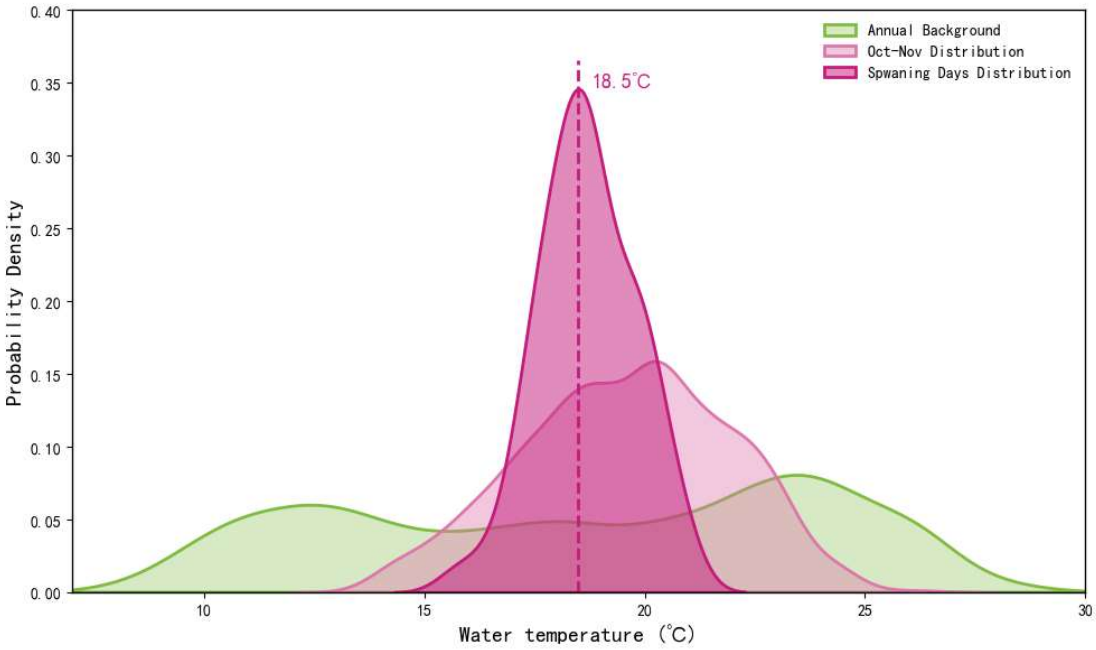
Figure 2. Temporal trend of spawning water temperature. The black dashed line represents the linear regression fit (slope = 0.0311 °C·yr^{-1}).

3.2. Estimation of the Optimal Gonadal Development and Spawning Water Temperature

Analysis of the overwintering temperature distributions (Figure 3a) revealed that the interannual mean of the period-averaged temperatures was 10.1 °C (range: 8.4–11.8 °C), the interannual means of the maximum and minimum temperatures were 11.6 °C (range: 10.1–13.4 °C) and 9.0 °C (range: 7.4–10.9 °C), respectively. According to the criteria defined in Section 2.2.3, this study identified 10.1 °C as the optimal mean temperature (O) for overwintering gonadal development, 11.6 °C as the upper thermal boundary (H), and 13.4 °C as the critical threshold beyond which temperatures should not rise (Figure 3a).



(a)



(**b**)

Figure 3. (**a**) Probability Density Distribution of Optimal Water Temperatures for Gonadal Development. For the overwintering period (January–February), three distribution curves were generated: the annual background temperature distribution, the overall January–February temperature distribution, and the distribution of January–February mean temperatures across years. (**b**) Probability Density Distribution of Optimal Water Temperatures for Spawning. For the spawning season, the following were constructed: the annual background temperature distribution, the overall October–November temperature distribution, and the distribution of temperatures on documented spawning dates.

The mean water temperature during historical spawning events was approximately 18.5 °C (Figure 3b), with the main span of the distribution ranging from 15.8 °C to 20.8 °C. Correspondingly, this study defined 20.8 °C as the upper limit for optimal spawning thermal conditions (Figure 3b).

Taken together, the distribution characteristics across both periods indicate that the thermal ranges associated with gonadal development and spawning are markedly narrower than the annual background water temperature range (7.4–29.7 °C). This contrast is particularly pronounced when comparing actual spawning temperatures with the background temperatures of October–November (13.4–26.6 °C), suggesting a specific thermal preference in this species.

3.3. Mismatch of Water Temperature with Species-Specific Thermal Optima Across Overwintering and Spawning Seasons

Based on the key temperature thresholds established in Section 3.2, daily water temperature heatmaps for the critical life-history periods spanning 1982–2023 were generated (Figure 4, left panels), and each daily temperature was classified into suitability zones (Figure 4, right panels) to evaluate the alignment between actual Yangtze River water temperatures and the thermal requirements of the species.

During the overwintering period, water temperatures were categorized into four suitability zones: cool (<10.1 °C), suitable (10.1–11.6 °C), warm (11.6–13.4 °C), and excessively warm (>13.4 °C). Noted that the overwintering window was extended to January–March due to the observed backward shift of cool temperatures (Figure 4a).

The heatmaps reveal that in 1999, water temperatures generally exceeded the upper thermal boundary (11.6 °C) for the first time, with temperatures surpassing the critical threshold (13.4 °C) in mid- to late March. The pronounced warming in 2007 caused water temperatures in early to mid-January to exceed 13.4 °C and those in late January to exceed 11.6 °C, resulting in the disappearance of the cool and suitable

thermal zones. This implies that if low temperatures serve as a necessary condition for initiating early gonadal development, January may no longer satisfy this requirement. After 2012, January–March water temperatures remained largely above 11.6 °C, and the overwintering thermal environment has since persisted in an excessively warm state throughout the year. By 2017, water temperatures for the first time exceeded 13.4 °C across nearly the entirety of January–March, indicating that from this period onward, the actual water temperatures of the Yangtze River may no longer meet the overwintering gonadal development requirements of Chinese sturgeon. Notably, transient temperature declines were observed in 2000 and during 2005–2006.

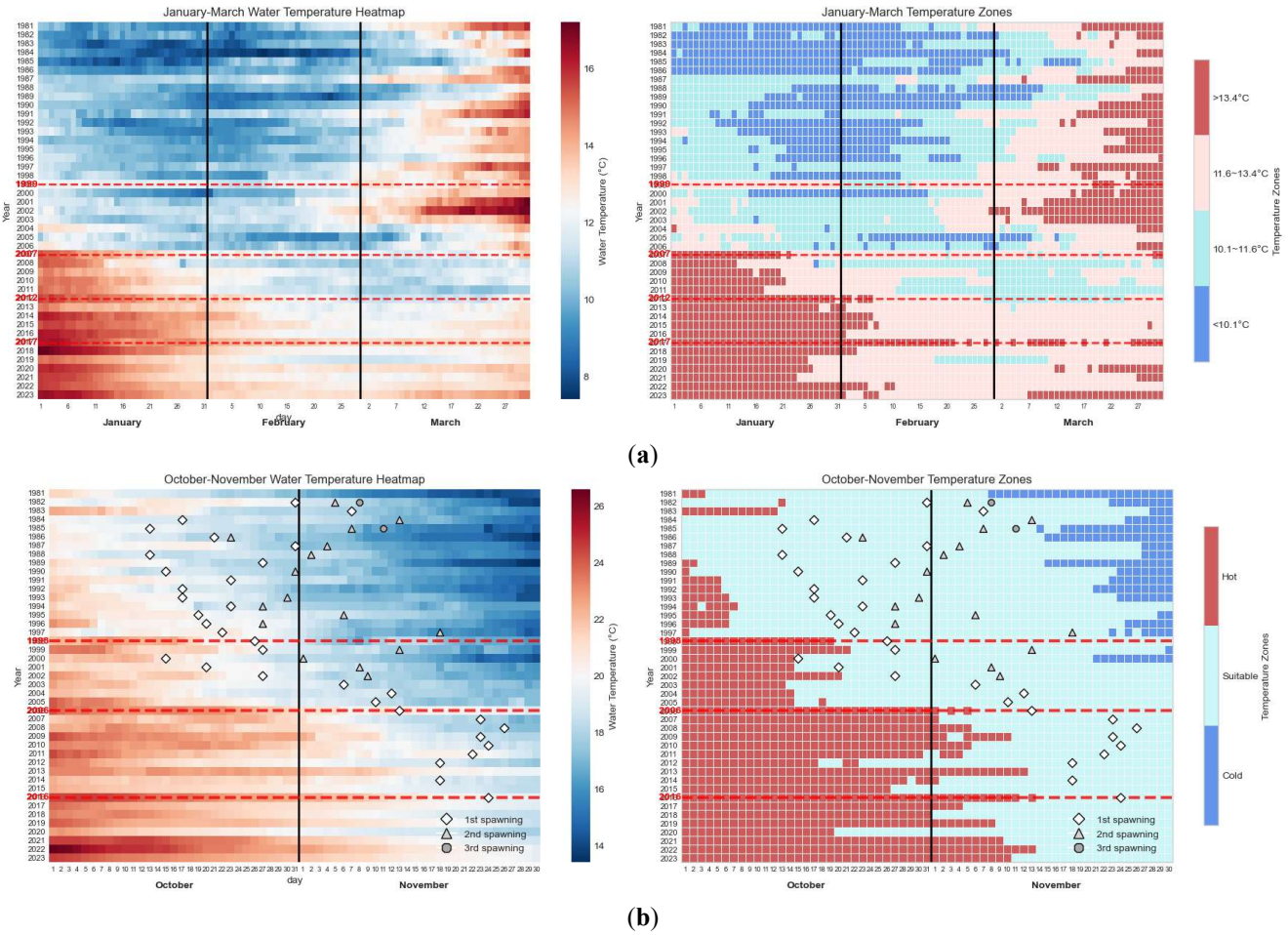


Figure 4. (**a**) Heatmaps of Water Temperature with Thermal Optima and Spawning Dates during Overwintering Seasons from 1981 to 2023. (**b**) Heatmaps of Water Temperature with Thermal Optima and Spawning Dates during Spawning Seasons from 1981 to 2023.

During the spawning season (October–November), water temperatures were classified into three suitability zones bounded by historical spawning temperature extremes: cool (<15.8 °C), suitable, and warm (>20.8 °C) (Figure 4b). Actual spawning dates were superimposed to enable simultaneous observation of interannual variations in spawning timing and thermal conditions. The analysis shows that warming around 1998 and 2006 had pronounced impacts: after 1998, thermal conditions in early to mid-October were no longer suitable for spawning; after 2006, the occurrence of suitable cool temperatures was further postponed until after early November. Examination of the spawning date distribution reveals a gradual backward shift since 1988, with a marked delay in the timing of the second spawning event by 1998. In 2003, the first spawning date was postponed to early to mid-November, and the second spawning event disappeared. By 2007, spawning dates were further delayed to mid- to late November. However, the postponement trend

was not monotonic: two periods of stalling or recovery occurred, coinciding with the temperature declines in 2000 and 2005, and synchronized with the cooling phases observed during the overwintering period.

3.4. Statistical Tests for Spawning Temperature Differences and Association Analysis of Spawning Dates Across Temporal Periods

The preceding analyses quantified the thermal requirements of the Chinese sturgeon at two critical stages, including overwintering and spawning, and examined the changing alignment between these requirements and the ambient thermal regime of the Yangtze River, suggesting an association between the arrival of suitable water temperatures and the occurrence of spawning events. In contrast to the inferred overwintering gonadal development period, spawning activity is documented with precise historical dates, an advantage that permits more refined analysis and statistical testing.

To further examine whether Chinese sturgeon have maintained a stable thermal preference for spawning under a changing thermal regime, and whether spawning dates within each period are synchronized with the arrival of suitable temperatures, the spawning samples were stratified into three periods based on years of pronounced thermal shifts, using 1998 and 2006 as boundaries. In addition, daily water temperatures during the same time window for 2017–2023 were extracted to serve as a reference for recent thermal conditions. Statistical comparisons of spawning dates and water temperatures were then conducted across these periods (Figure 5).

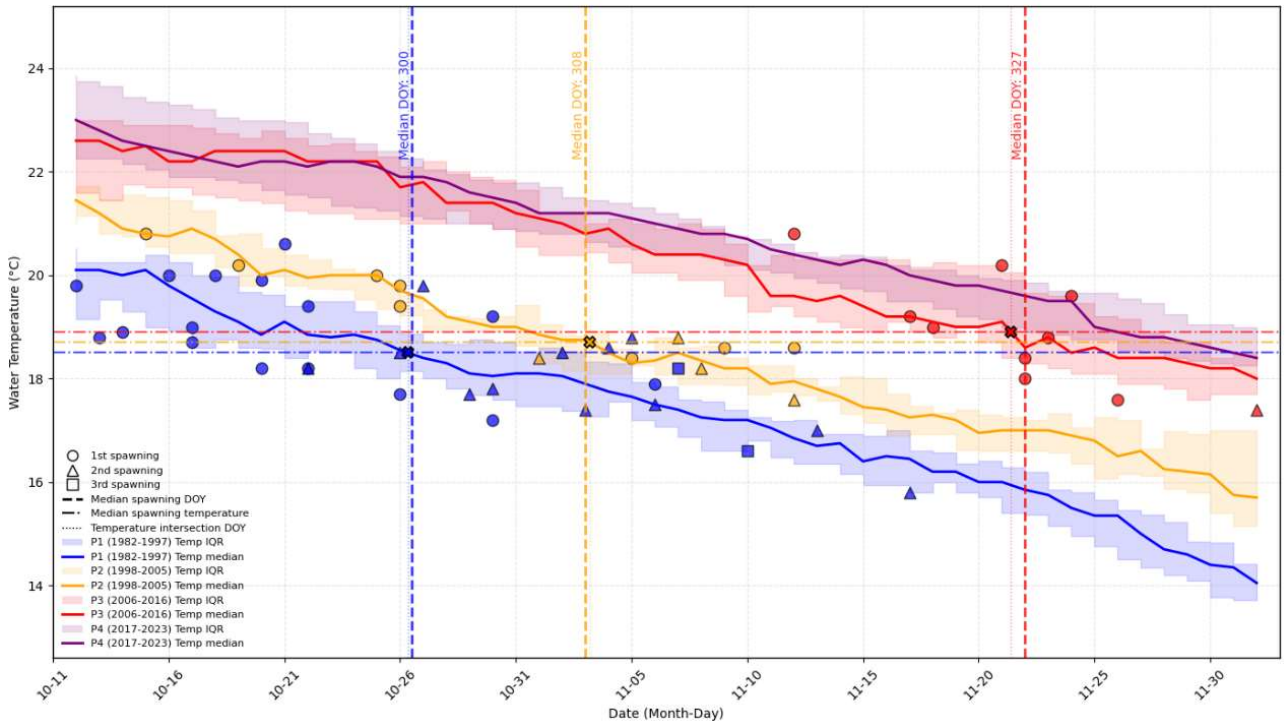


Figure 5. Median Distribution of Water Temperature and Spawning Dates Across Periods IQR band and Median Trajectory present the overall daily thermal variability in four periods, dotted lines and intersection points indicate median spawning dates, and the intersection dates between the seasonal cooling curve and the suitable temperature threshold for each period, respectively.

The results (Table 1) showed significant differences in daily water temperatures among the four periods, indicating a persistent and pronounced warming trend in the thermal background during the spawning season. Extremely small *p*-values showed that the differences between P1 and P3, P1 and P4, P2 and P3, and P2 and P4 were all highly significant. The comparison between P3 and P4 remained significant but with a *p*-value several orders of magnitude larger, possibly suggesting either a deceleration of warming after 2016 or increased interannual variability.

Table 1. Pairwise water temperature comparisons (Mann-Whitney U) across periods.

Period A	Period B	U Statistic	*p*-Value	Significant ($p < 0.05$)
P1 (1982–1997)	P2 (1998–2005)	117,819.5	3.41×10^{-20}	True
P1 (1982–1997)	P3 (2006–2016)	49,398	7.82×10^{-141}	True
P1 (1982–1997)	P4 (2017–2023)	22,070	1.67×10^{-122}	True
P2 (1998–2005)	P3 (2006–2016)	48,350	2.74×10^{-57}	True
P2 (1998–2005)	P4 (2017–2023)	24,860	4.97×10^{-59}	True
P3 (2006–2016)	P4 (2017–2023)	94,985.5	2.37×10^{-2}	True

In stark contrast to this continuous rise in background water temperatures, spawning water temperatures among the three periods showed no significant differences (Table 2, $p > 0.139$ for all pairwise comparisons). The median spawning temperature remained stable at approximately 18.5 °C, supporting the existence of a stable species-specific spawning temperature preference. It should be noted that the slight increasing trend was observed in the median spawning temperatures across the three periods (18.5 → 18.7 → 18.9 °C, Table 3). Nonetheless, this trend may reflect the environmental stress of rising water temperatures.

Table 2. Two-tailed Mann-Whitney U Test Results of Spawning Date and Water Temperature.

Compared Groups	Spawning Date (DOY)	Spawning WT (°C)
P1 (1981–1997):P2 (1998–2005)	U = 129.0, $p = 0.1593$	U = 126.5, $p = 0.1394$
P2 (1998–2005):P3 (2006–2016)	U = 1.0, $p = 0.0001$	U = 65.0, $p = 0.7661$
P1 (1981–1997):P3 (2006–2016)	U = 2.0, $p < 0.0001$	U = 119.5, $p = 0.3483$

Meanwhile, spawning dates (DOY) exhibited highly significant stepwise delays across periods, with $p < 0.001$ for the comparison between P2 and P3, and between P1 and P3. More importantly, the median spawning date within each period (P1: 300, P2: 308, P3: 327) corresponded closely with the date on which the seasonal cooling trajectory intersected the period-specific median spawning temperature (P1: 300.3, P2: 308.2, P3: 326.4, Table 3). The progressive delay in spawning dates closely mirrored the postponement of the thermal cue date, reflecting the tight coupling between reproductive phenology and ambient thermal conditions. Given that water temperature and calendar date are independent dimensions, this persistent, period-transcending synchrony strongly suggests that the seasonal decline in water temperature to approximately 18.5 °C likely constitutes a necessary cue for triggering spawning in Chinese sturgeon. The pronounced delay in spawning dates is thus fundamentally attributable to the postponement of the annual timing at of this thermal cue.

Table 3. Metrics and Synchrony: Mean & Median Spawning Dates and Water Temperature.

	Spawning Date (DOY)		Spawning WT (°C)		
	Avg.	Mdn.	Avg.	Mdn.	Date
P1	301.2, 95%CI = (297.6–304.8)	300, IQR = (294–309)	18.5, 95%CI = (18.0–18.9)	18.5, IQR = (17.7–19.1)	300.3
P2	305.8, 95%CI = (299.8–311.8)	308, IQR = (300–313)	19.1, 95%CI = (18.5–19.7)	18.7, IQR = (18.4–19.9)	308.2
P3	326.7, 95%CI = (322.8–330.6)	327, IQR = (324–329)	18.9, 95%CI = (18.1–19.7)	18.9, IQR = (18.1–19.5)	326.4

4. Discussion

4.1. Coupling Mechanisms of Thermal Mismatch: Combined Effects of Loss of Overwintering Low-Temperature and Delayed Autumn Cooling

Through a systematic analysis of water temperatures during the overwintering and spawning periods of Chinese sturgeon, this study reveals a coupled amplification mechanism of thermal mismatch along the reproductive chain. Heatmap analyses show that thermal mismatches at these two critical stages exhibited a consistent deteriorating trend. The sustained increase in overwintering water temperatures may impair

gonadal development, while the progressively postponed timing of autumn cooling may compress the effective spawning window. The superposition of these two mismatches leads to the fact that, on the one hand, broodstock arriving at the spawning grounds may fail to complete adequate gonadal maturation; on the other hand, even if some broodstock complete gonadal development, the delayed autumn cooling exposes them to higher energy expenditure and environmental risks while awaiting suitable temperatures. This coupling mechanism plausibly explains why the reproductive decline of Chinese sturgeon has followed a stepped pattern rather than a monotonic trend. When the mismatch at either stage accumulates to a critical level, the entire reproductive chain may break down.

Notably, two transient recovery periods were identified in the time series of spawning dates around 2000 and 2005 to 2006, during which the first spawning dates advanced or stabilized, exhibiting a high degree of synchrony with the water temperatures change during both the gonadal development and spawning periods. This further supports the inference of coupling mechanisms: simultaneous improvements in thermal conditions at both overwintering and spawning stages can temporarily alleviate reproductive stress.

4.2. Stability of Spawning Temperature and Adherence to the Temporal Dynamic Signal

Although pairwise Mann-Whitney U tests revealed significant warming trends in ambient water temperatures during the spawning season, spawning water temperatures showed no significant differences among periods (all comparisons $p > 0.139$), with median spawning temperatures remaining consistently around 18.5 °C (P1: 18.5 °C, P2: 18.7 °C, P3: 18.9 °C) over more than three decades. This remarkable stability indicates that Chinese sturgeon possess a fixed spawning thermal preference that has not shifted with environmental warming. For ectothermic organisms, physiological thermal optima are typically constrained by biochemical and biophysical properties such as enzyme kinetics and membrane fluidity, and are unlikely to undergo genetic-level changes over short timescales [41]. Therefore, the absence of a significant shift in spawning temperature preference is more likely to reflect physiological constraint than active adaptation.

However, the calendar date on which autumn water temperatures decline to this threshold has been progressively postponed. Our intersection analysis revealed that the date when the period-specific median cooling curve crossed the median spawning temperature closely matched the actual median spawning date within each period. This indicates that the delay in spawning dates is not a result of active phenological adjustment by Chinese sturgeon, but rather a passive response to the delayed thermal cue: the spice still waits for the optimal water temperature, but this condition occurs increasingly later each year.

4.3. Limitations

This study has several limitations. First, the thermal thresholds identified are based on statistical associations with historical spawning events rather than direct physiological measurements. Controlled experiments on Chinese sturgeon are needed to confirm the causal relationships between specific temperature regimes and gonadal development and spawning success.

Second, owing to the lack of direct observations on the population dynamics of the Chinese sturgeon spawning stock, this study cannot quantitatively partition the relative contributions of thermal stress versus decline in broodstock abundance to the cessation of reproduction. The interaction between population size and thermal suitability requires further investigation through integrated population modeling.

Finally, while the Yichang Hydrological Station is the best available proxy for thermal conditions at the spawning ground, it may not fully capture fine-scale spatial heterogeneity across different microhabitats within the spawning area.

4.4. Conservation Implications

With continued climate warming, proactive management of reservoir thermal regimes will become increasingly critical for creating the frequency and persistence of the aligned conditions for reproduction of Chinese Sturgeon. Given that thermal mismatches have accumulated cumulative effects along the reproductive chain, conservation interventions should cover the entire reproductive cycle rather than focusing solely on the spawning season. Ecological flow regulation or localized cooling interventions that appropriately advance the timing of suitable water temperatures could help restore synchrony with the species' reproductive phenology.

Furthermore, given the positive feedback reinforcement between population decline and thermal stress, relying solely on thermal environment improvement may be insufficient for population recovery. While restoring thermal suitability, complementary population supplementation and protection measures, such as captive breeding and release, habitat restoration, and shipping disturbance control, must be pursued simultaneously [42].

5. Conclusions

This study provides a quantitative assessment of the thermal mismatches underlying the stepped reproductive failure of Chinese sturgeon in the Yangtze River. Based on kernel density estimation (KDE), the upper boundary for overwintering gonadal development was approximately 11.6 °C, with a critical threshold of approximately 13.4 °C. The median spawning temperature was approximately 18.5 °C, with an upper limit of approximately 20.8 °C. These thresholds constitute quantitative benchmarks for assessing the suitability of the thermal regime for Chinese sturgeon reproduction.

Our analysis reveals that the evolution of thermal mismatch exhibits stepped characteristics, with three critical nodes identified. During 1998 to 1999, overwintering water temperatures first widely exceeded the 11.6 °C upper boundary. During 2006 to 2007, the suitable low-temperature zone for January to March largely disappeared. After 2017, daily water temperatures almost entirely surpassed the 13.4 °C critical threshold, marking the complete loss of overwintering low-temperature conditions. The coupled amplification effect along the reproductive chain provides an explanation for the stepped deterioration of Chinese sturgeon reproduction, from occasional spawning anomalies to complete interruption.

Spawning water temperatures remained stable at approximately 18.5 °C over more than three decades, but the date of autumn cooling to this temperature was progressively delayed by a cumulative total of approximately 27 days. Intersection analysis showed that actual spawning dates were almost perfectly synchronized with the date when the cooling curve crossed the median spawning temperature, suggesting that the spawning delay is a passive consequence of postponed thermal signals.

Collectively, the results unequivocally demonstrate that the current thermal regime of the Yangtze River has systematically deviated from the conditions required for successful reproduction of Chinese sturgeon, and that this objectively existing environmental stress is continuing to intensify.

Supplementary Materials

The following supporting information can be found at: https://www.sciepublish.com/article/pii/1262, Figure S1: Changes of Spawning Grounds for Chinese Surgeon.

Author Contributions

Conceptualization, X.N.; Methodology, J.C. and X.N.; Software, X.N.; Validation, X.N. and D.L.; Formal Analysis, X.N.; Investigation, J.C. and X.N.; Resources, J.C.; Data Curation, J.C. and X.N.; Writing—Original Draft Preparation, X.N.; Writing—Review & Editing, J.C. and D.L.; Visualization, X.N.; Supervision, J.C.; Project Administration, J.C. and D.L.; Funding Acquisition, J.C.

Ethics Statement

Not applicable.

Informed Consent Statement

Not applicable.

Data Availability Statement

The data on the egg-laying days covered in this study has been cited from relevant literature in the text. The water temperature data was sourced from the hydrological station and the author is not authorized to share.

Funding

This research was funded by the National-Key R&D Program of China (No. 2022YFC3204200) and the project of ChinaThree Gorges Corporation (202203404).

Declaration of Competing Interest

The authors declare that they have no known competing financial interests or personal relationships that could have appeared to influence the work reported in this paper.

References

1. Chang J. Structure and Dynamics of the Spwaning Stock of Chinese Sturgeon, *Acipenser sinensis*, in Yangtze River. Ph.D. Dissertation, Insititute of Hydrobiology, Chinese Academy of Sciences, Wuhan, China, 1999.
2. Gao X, Lin P, Li M, Duan Z, Liu H. Impact of the Three Gorges Dam on the spawning stock and natural reproduction of Chinese sturgeon in Changjiang River, China. *Chin. J. Oceanol. Limnol.* **2016**, *34*, 894–901. DOI:10.1007/s00343-016-5027-z
3. Gao X, Lin P, Li M, Duan Z, Liu H. Effects of Water Temperature and Discharge on Natural Reproduction Time of the Chinese Sturgeon, *Acipenser sinensis*, in the Yangtze River, China and Impacts of the Impoundment of the Three Gorges Reservoir. *Zool. Sci.* **2014**, *31*, 274–278. DOI:10.2108/zs130123
4. The Changjiang Aquatic Resources Survey Group, Sichuan Province. *The Biology of the Sturgeons in Changjiang and Their Artificial Propagation*; Sichuan Scientific and Techinical Publishing House: Chengdu, China, 1988.
5. Jiao W. Impact of Three Gorges Project on the Population Dynamics of Chinese Sturgeon (*Acipenser Sinensis*) in the Yangtze River. Ph.D. Dissertation, Univerdity of Chinese Academy of Science, Wuhan Botanical Garden, Chinese Academy of Science, Wuhan, China, 2020.
6. Liao X, Zhu B, Chang J. Study on Conservation of Chinese Sturgeon. *Yangtze River* **2017**, *48*, 16–20+35. DOI:10.16232/j.cnki.1001-4179.2017.11.004
7. Stearns SC. *The Evolution of Life Histories*; Oxford University Press: Oxford, UK, 1992.
8. Poff N, Allan JD, Bain M, Karr J, Prestegaard K, Richter B, et al. The Natural Flow Regime. *BioScience* **2014**, *47*, 769–784. DOI:10.2307/1313099
9. Stearns SC. A New View of Life-History Evolution. *Oikos* **1980**, *35*, 266–281. DOI:10.2307/3544434
10. Thackeray SJ, Henrys PA, Hemming D, Bell JR, Botham MS, Burthe S, et al. Phenological sensitivity to climate across taxa and trophic levels. *Nature* **2016**, *535*, 241–245. DOI:10.1038/nature18608
11. Bunn S, Arthington A. Basic Principles and Ecological Consequences of Altered Flow Regimes for Aquatic Deflation Basin Lakes. *Environ. Manag.* **2002**, *30*, 492–507. DOI:10.1007/s00267-002-2737-0
12. Goodman BJ, Guy CS, Camp SL, Gardner WM, Kappenman KM, Webb MAH. Shovelnose sturgeon spawning in relation to varying discharge treatments in a missouri river tributary. *River Res. Appl.* **2013**, *29*, 1004–1015. DOI:DOI:10.1002/rra.2587
13. Junk WJ, Bayley P, Sparks R. The Flood Pulse Concept in River-Floodplain Systems. *Can. Spec. Publ. Fish. Aquat. Sci.* **1989**, *106*, 110–127.
14. Rochard E, Castelnaud G, Lepage M. Sturgeons (Pisces: Acipenseridae); threats and prospects. *J. Fish Biol.* **1990**, *37*, 123–132. DOI:10.1111/j.1095-8649.1990.tb05028.x

15. Beamesderfer RCP, Farr RA. Alternatives for the protection and restoration of sturgeons and their habitat. In *Sturgeon Biodiversity and Conservation*; Birstein VJ, Waldman JR, Bemis WE, Eds.; Springer: Dordrecht, The Netherlands, 1997; pp. 407–417. DOI:10.1007/0-306-46854-9_29
16. Bruch R, Binkowski F. Spawning behavior of Lake Sturgeon (*Acipenser fulvescens*). *J. Appl. Ichthyol.* **2002**, *18*, 570–579. DOI:10.1046/j.1439-0426.2002.00421.x
17. Kieffer M, Kynard B. Spawning of the Shortnose Sturgeon in the Merrimack River, Massachusetts. *Trans. Am. Fish. Soc.* **1996**, *125*, 179–186. DOI:10.1577/1548-8659(1996)125%3C0179:SOTSSI%3E2.3.CO;2
18. Dettlaff TA, Ginsburg AS, Schmalhausen OI. *Developmental Biology and Aquaculture*; Springer: Berlin/Heidelberg, Germany, 2012.
19. Chebanov M, Galich E. *Sturgeon Hatchery Manual*; FAO Fisheries and Aquaculture Technical Paper; Food and Agriculture Organization of the United Nations: Rome, Italy, 2011.
20. Dettlaff TA, Davydova SI. Differential sensitivity of cells of follicular epithelium and oocytes in the stellate sturgeon to unfavorable conditions, and correlating influence of triiodothyronine. *Gen. Comp. Endocrinol.* **1979**, *39*, 236–243. DOI:10.1016/0016-6480(79)90228-4
21. Williot P, Brun R, Rouault T, Rooryck O. Management of female spawners of the *Siberian sturgeon*, *Acipenser baeri* Brandt: first results. In *Acipenser: Actes du premier colloque international sur l'esturgeon, Bordeaux, 3–6 Octobre 1989*; Cemagref Editions: Paris, France, 1991; pp. 365–379.
22. Van Eenennaam J, Chapman F, Jarvis P. Aquaculture. In *Sturgeons and Paddlefish of North America*; Springer: Berlin/Heidelberg, Germany, 2004; pp. 277–311. DOI:10.1007/1-4020-2833-4_14
23. Webb MAH, Van Eenennaam JP, Doroshov SI, Moberg GP. Preliminary observations on the effects of holding temperature on reproductive performance of female white sturgeon, *Acipenser transmontanus* Richardson. *Aquaculture* **1999**, *176*, 315–329. DOI:10.1016/S0044-8486(99)00108-8
24. Webb MAH, Van Eenennaam JP, Feist GW, Linares-Casenave J, Fitzpatrick MS, Schreck CB, et al. Effects of thermal regime on ovarian maturation and plasma sex steroids in farmed white sturgeon, *Acipenser transmontanus*. *Aquaculture* **2001**, *201*, 137–151. DOI:10.1016/S0044-8486(01)00550-6
25. Yang D, Kynard B, Wei Q, Chen X, Zheng W, Du H. Distribution and movement of Chinese sturgeon, *Acipenser sinensis*, on the spawning ground located below the Gezhouba Dam during spawning seasons. *J. Appl. Ichthyol.* **2007**, *22*, 145–151. DOI:10.1111/j.1439-0426.2007.00943.x
26. Gao X, Li M-Z, Lin P-C, Duan Z-H, Liu H-Z. Environmental cues for natural reproduction of the Chinese sturgeon, *Acipenser sinensis* Gray, 1835, in the Yangtze River, China. *J. Appl. Ichthyol.* **2013**, *29*, 1389–1394. DOI:10.1111/jai.12363
27. Chang T, Gao X, Danley PD, Lin P, Li M, Liu H. Longitudinal and temporal water temperature patterns in the Yangtze River and its influence on spawning of the Chinese sturgeon (*Acipenser sinensis* Gray 1835). *River Res. Appl.* **2017**, *33*, 1445–1451. DOI:DOI:10.1002/rra.3210
28. Tao Y, Wang Y, Rhoads B, Wang D, Ni L, Wu J. Quantifying the impacts of the Three Gorges Reservoir on water temperature in the middle reach of the Yangtze River. *J. Hydrol.* **2020**, *582*, 124476. DOI:10.1016/j.jhydrol.2019.124476
29. Shen Y, Wang P, Wang C, Yu Y, Kong N. Potential causes of habitat degradation and spawning time delay of the Chinese sturgeon (*Acipenser sinensis*). *Ecol. Inform.* **2018**, *43*, 96–105. DOI:DOI:10.1016/j.ecoinf.2017.11.002
30. Zhang P, Qiao Y, Grenouillet G, Lek S, Cai L, Chang J. Responses of spawning thermal suitability to climate change and hydropower operation for typical fishes below the Three Gorges Dam. *Ecol. Indic.* **2021**, *121*, 107186. DOI:10.1016/j.ecolind.2020.107186
31. Zhang H, Kang M, Wu J, Wang C, Li J, Du H, et al. Increasing River Temperature Shifts Impact the Yangtze Ecosystem: Evidence from the Endangered Chinese Sturgeon. *Animals* **2019**, *9*, 583. DOI:10.3390/ani9080583
32. Xiao H, Duan Z-H. Hydrological and water chemical factors in the Yichang reach of the Yangtze River pre- and post-impoundment of the Three Gorges Reservoir: Consequences for the Chinese sturgeon *Acipenser sinensis* spawning population (a perspective). *J. Appl. Ichthyol.* **2011**, *27*, 387–393. DOI:10.1111/j.1439-0426.2011.01745.x
33. Deng Z, Xu Y, Zhao Y. Anaysis on *Acipenser sinensis* spawning ground and spawning scales below Gezhouba dam by means of examiningthe digestive contents of benthic fishes. In *Acipenser*; Williot P, Ed.; Cemagref-Discova Pub: Paris, France, 1991; pp. 243–250.
34. Yu Z, Zhou C, Deng Z, Xu Y, Xiang Y. Investigation on natural reproduction of Chinese sturgeon downstream of Gezhouba Junction. *J. Hydroecol.* **1983**, *2*, 2–4. DOI:10.15928/j.1674-3075.1983.02.002
35. Qiao Y, Tang X, Brosse S, Chang J. Chinese Sturgeon (*Acipenser sinensis*) in the Yangtze River: A hydroacoustic assessment of fish location and abundance on the last spawning ground. *J. Appl. Ichthyol.* **2006**, *22*, 140–144. DOI:10.1111/j.1439-0426.2007.00942.x

36. Tao J, Qiao Y, Yang Z, Chang J, Dong F, Wan L. Estimation on the Spawning Population and Spawning Sizes of Chinesesturgeon (*Acipenser sinensis*) and Trend Analysis of Their Change in Recent Years. *J. Hydroecol.* **2009**, *30*, 37–43. DOI:10.15928/j.1674-3075.2009.02.016
37. Rosenblatt M. Remarks on Some Nonparametric Estimates of a Density Function. *Ann. Math. Stat.* **1956**, *27*, 832–837. DOI:10.1214/aoms/1177728190
38. Parzen E. On Estimation of a Probability Density Function and Mode. *Ann. Math. Stat.* **1962**, *33*, 1065–1076. DOI:10.1214/aoms/1177704472
39. Scott DW. Kernel Density Estimators. In *Multivariate Density Estimation*; Wiley Series in Probability and Statistics; Wiley: Hoboken, NJ, USA, 2015; pp. 137–216. DOI:10.1002/9781118575574.ch6
40. Mann HB, Whitney DR. On a Test of Whether one of Two Random Variables is Stochastically Larger than the Other. *Ann. Math. Stat.* **1947**, *18*, 50–60. DOI:10.1214/aoms/1177730491
41. Pörtner HO, Farrell AP. Physiology and Climate Change. *Science* **2008**, *322*, 690–692. DOI:10.1126/science.1163156
42. Chang T, Gao X, Liu H. Potential hydrological regime requirements for spawning success of the Chinese sturgeon *Acipenser sinensis* in its present spawning ground of the Yangtze River. *Ecohydrology* **2021**, *14*, e2339. DOI:DOI:10.1002/eco.2339